Paper 114

Proceedings of the Eleventh International Conference
on Computational Structures Technology,
B.H.V. Topping, (Editor),
Civil-Comp Press, Stirlingshire, Scotland

Train-Bridge Interaction and Fatigue on Railway Bridges

A. Bekö and L. Rossbacher
Special Structures and Dynamics
Vienna Consulting Engineers, Austria

Abstract

This paper addresses various aspects of a fatigue analysis.. Initially a finite element model of a historical riveted railway bridge, the Salzach-brücke, was created. The structure was selected since cracks had been observed on some of its cross-girders. The Salzach Bridge, built in 1907, is a classical example of a riveted truss bridge. In order to study the influence of the full train-bridge interaction on the structure's response, a precise three dimensional model of an ICE3 type of train was developed. To run a two system interaction in ANSYS a built-in solution is to use constraint equations. To verify this approach a user implemented iterative solution scheme has been developed. After comparison of the results of the two approaches the constraint equation method is used to run the full analysis. The stress histories (axial and shear) for the cross-girder are extracted and N-S curves are calculated using the rainflow algorithm.

Keywords: riveted bridge, train-bridge interaction, fatigue, rainflow counting, field data.

1 Introduction

The structure investigated in this study is an old railway bridge in Austria. It lies on the track Salzburg-Wörgl at km 68.80. It crosses over the river Salzach and is located near the town of Schwarzach im Pongau in the province of Salzburg. It was built between 1905 and 1907 and was reconditioned in 1965. It is a riveted truss bridge with a span of 40 meters, a construction height of 4.30 meters and a width of 3.00 meters. The bridge's construction material is a form of alkaline low carbon "mild" steel originally called: *basisches Martin-Flusseisen*.

The structure was investigated as it has developed well visible cracks on five out of its eleven cross-girders. The intention is to qualify this damage and assess whether it could have been caused by fatigue or rather by inappropriate detailing.

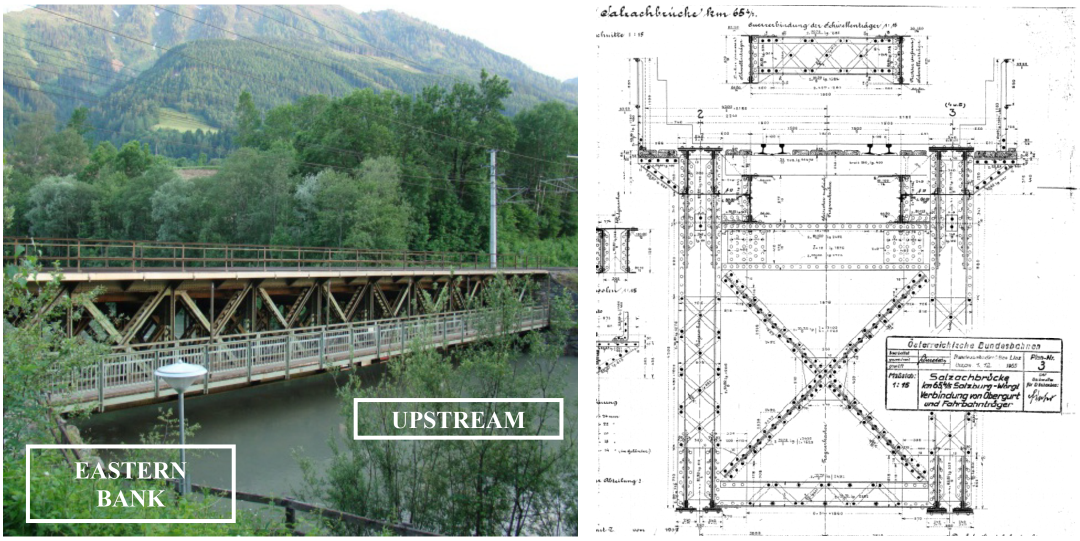

Figure 1: The Salzach bridge, cross-section of bridge (original blueprint).

A test programme was conducted to retrieve modal data for the bridge. The choice of sensor positions was such that the global and local structural behaviour could be analysed both in vertical and horizontal directions. Altogether fourteen sensors were used and three measurements with three different layouts were performed. In all three layouts eleven of these sensors were placed along the bridge on the overhanging pedestrian walkway on the side of the main truss. The remaining three sensors were placed on the steel plates of the truss joints under the top deck or at the downstream side. These sensors provided information about the torsional motion of the bridge. The data was then evaluated to extract actual modal parameters of the structure.

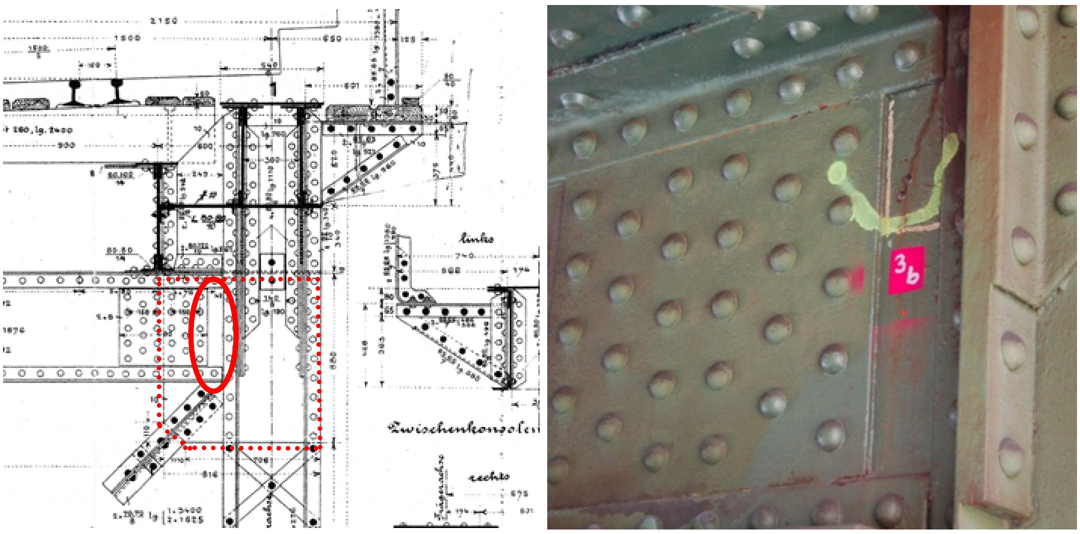

Figure 2: Detail of the connection between cross-girder and vertical main beam with damaged element highlighted in red. Crack location marked by ellipse. Detail photograph of the damage at position U03.

Figure 3: Brimos wireless on the walkway. EpiSensor on the joint.

2 Modelling

2.1 Bridge

The geometry was taken from the design drawings. The numerical analysis was performed with the commercial finite element code ANSYS (SAS IP). A numerical model representing the three-dimensional mass and stiffness distribution of the bridge was used. The wooden sleepers were introduced to the model to simulate the connection of the rails to the bridge more precisely. The rails were modeled along the length of the bridge, plus 400m before and after it to facilitate a full transient train-track interaction analysis. The connection of the rails to the sleepers was assumed rigid.

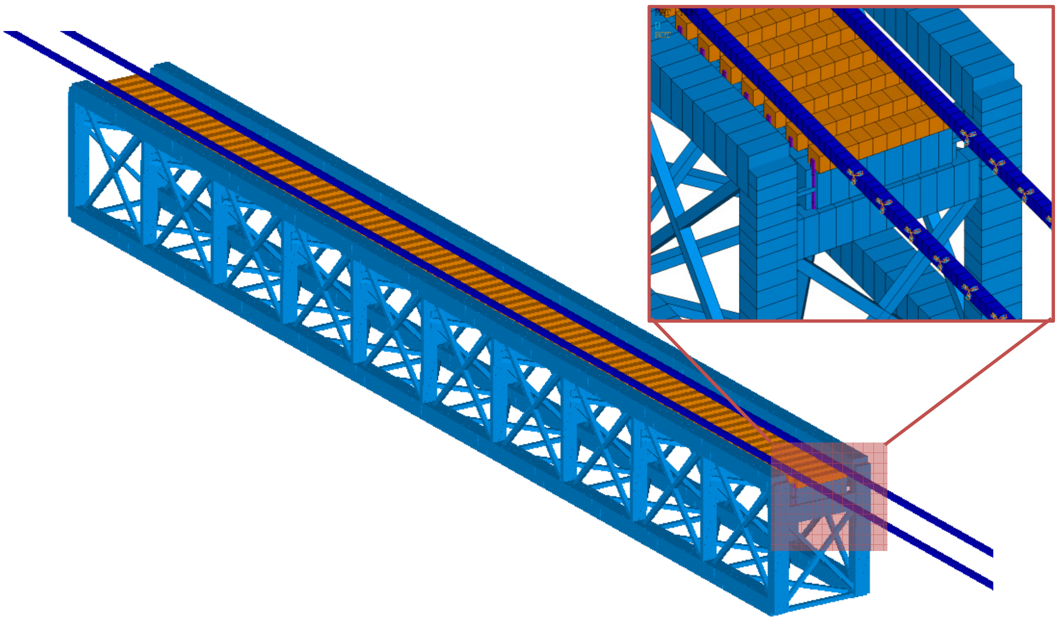

Figure 4: Axonometric view of the solid model with details of off-bridge track support.

In order to accurately describe the torsion behavior of the structure and the distribution of the vertical loads, the non-structural mass (pedestrian walkway) is dispersed over the upstream bottom chord of the bridge modeled by MASS21 elements.

Upon referencing historical books of the time the elastic module for the structural mild steel was assumed with the value of 155000 N/mm^2. The elastic modulus for the steel rails was set to 210000 N/mm^2. The mass per unit volume of both materials was assumed as 7850 kg/m^3.

The actual supports of the bridge had to be checked on site. There are fixed supports at the east bank while the west bank supports are movable in the longitudinal direction. Moreover, the bridge is supported at the bottom chords only.

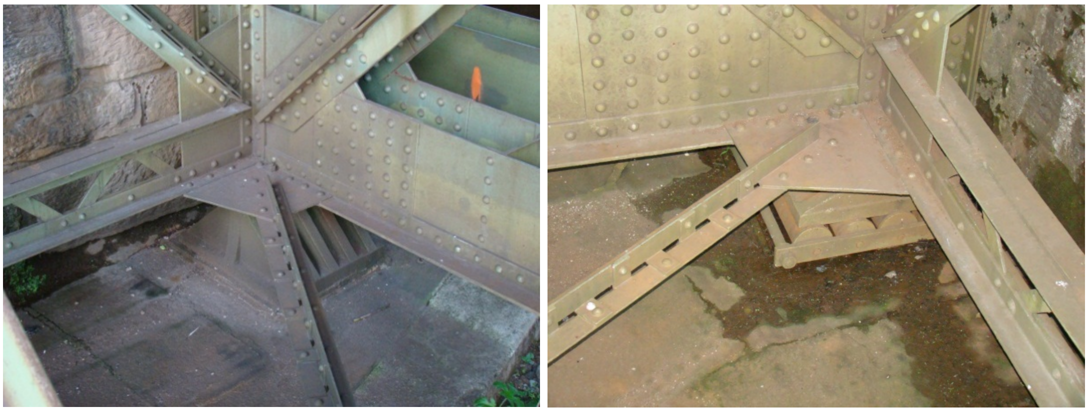

Figure 5: Supports of the bridge at the east (left) and west (right) ends.

In the table below the numerical eigenfrequencies are compared to the test results. They show an acceptable agreement which means the model can be used for further analysis. For the last entry of the table it was difficult to find a unison match. The two closest numerical modes could both harmonize with the experimental frequency as this was identified as a combination of horizontal and vertical bending and torsion.

	Mode shapes	**Numerical [Hz]**	**Test [Hz]**
1	1. vertical bending	4.78	4.79
2	3. horizontal bending	12.74	12.96
3	2. vertical bending	15.76	15.54
4	4. horizontal bending / torsion	18.23 / 19.76	19.26

Table 1: Comparison of numerical and test natural frequencies.

After careful matching of the numerical and tested modes a final graphical comparison is presented in the next figure.

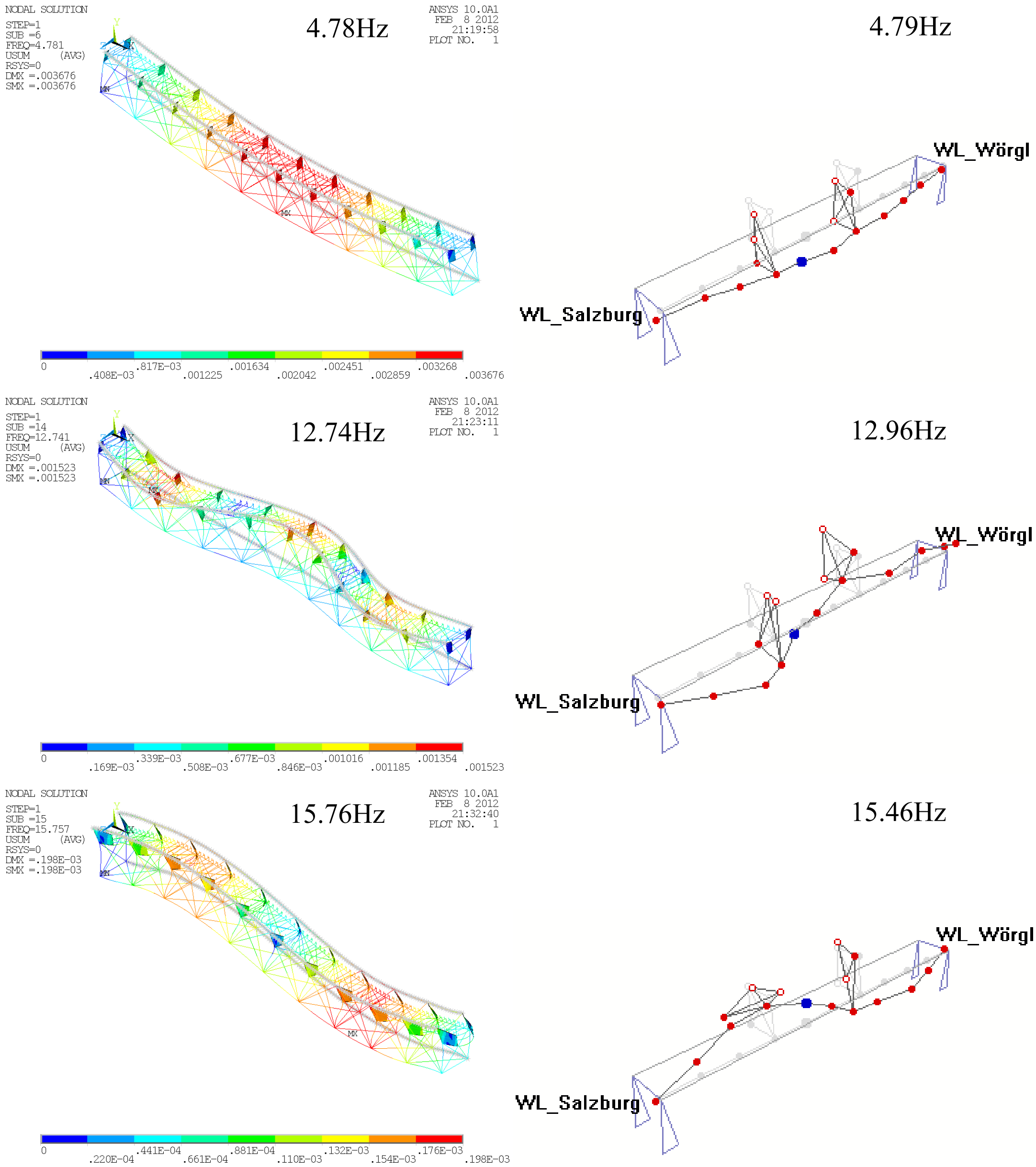

Figure 6: Comparison of numerical and experimental mode shapes.

2.2 Train

For the transient analysis we chose to model an ICE 3 train based on an available detailed description. Although the very same type of train does not operate on this line it is comparable to the passenger trains operated on the line and so can yield a realistic picture about the loading of the bridge. The dimensions of the locomotive and the in-between carriages are given in Figure 7. The model was built in ANSYS Structural by APDL.

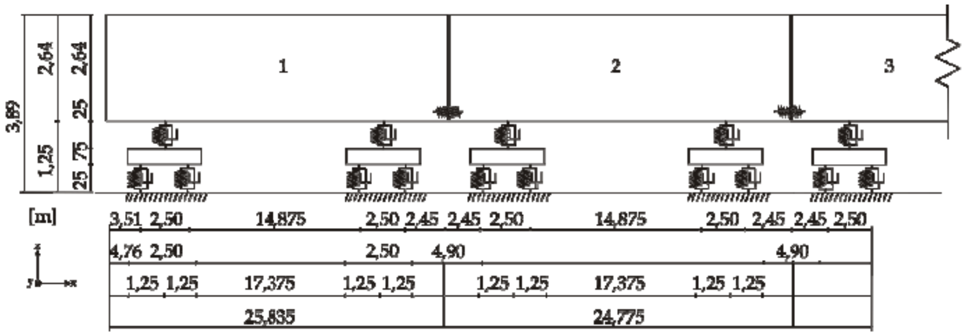

Figure 7: ICE 3 train length properties.

The total length of the ICE3 train with 16 carriages is 393.70m. The whole mass of the reference vehicle (train plus max. loading) is 992.64 tons. The mass per meter is approximately 2.5 t/m and axle loads range from 142.50kN up to 170.9kN.

In the numerical Model of the ICE3 train the coaches are approximated by rigid bodies. These rigid bodies are modelled by BEAM44 elements which were assigned a stiff material. The mass of the ICE3 train is distributed on the horizontal BEAM44 elements only. The longitudinal coupling between the coaches is simulated with COMBIN14 spring elements with the stiffness of 10kN/mm.

Also the bogies of the train were modelled. In Figure 8 the principle of the numerical modelling is shown. A Hertzian spring [1] represents the contact between the rail and the wheel. The mass of the wheels is modelled by MASS21 elements. The damping of the primary and secondary springs was assumed with the value of 1kN at 0.1m/s.

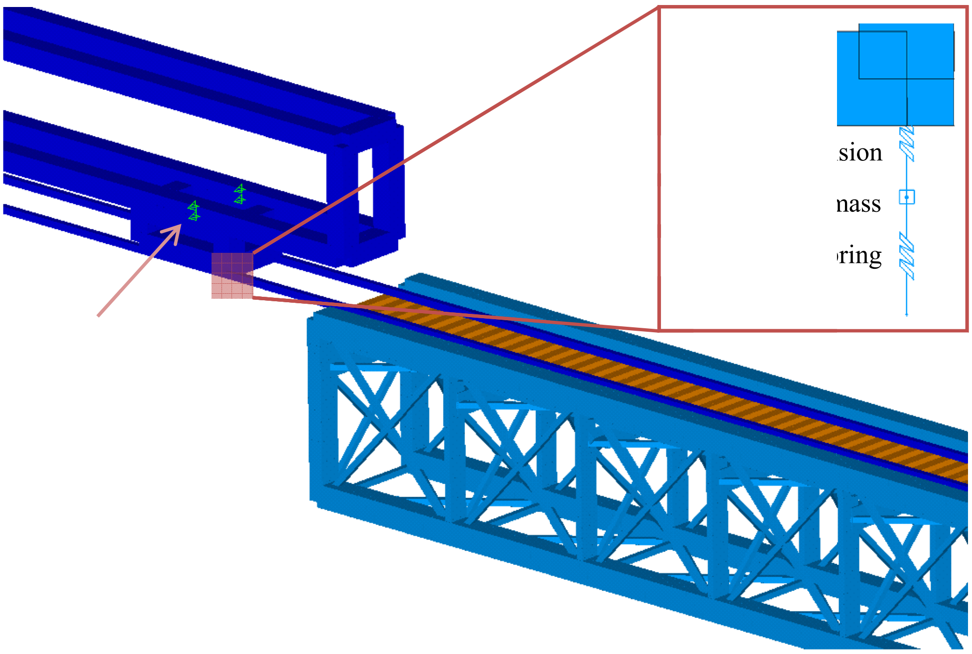

Figure 8: Train model placed on tracks. Detail of wheel suspension.

3 Solution

The train passes the bridge with a velocity of 120km/h. Various time stepping has been used to get a comparison of the output and an indication of the necessary step size. The time step of 0.002s equals to a forward displacement of 6.67cm. With an element size of about 15cm this is the lowest allowable time step already allowing the tying of the wheel node to the same node of the rail in two consecutive time steps. The results show that this phenomenon does not have significant influence on the results as compared to the time step of 0.005s.

The analysis was solved with the Newmark time integration scheme. An overall damping of 3% was applied.

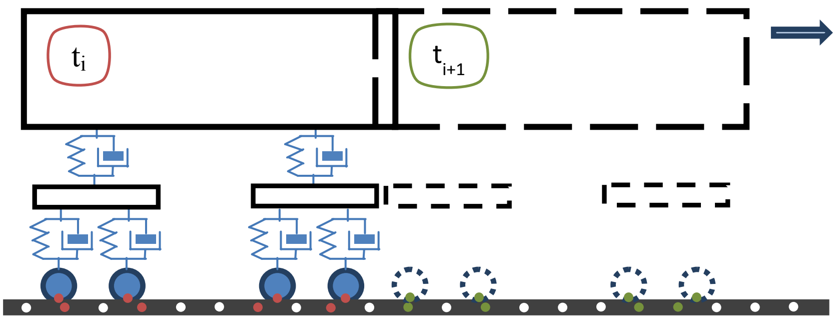

Figure 9: Scheme of the connection between rail and wheel nodes in each time step by constraint equations. The contact nodes of the wheels are constrained to have the same vertical displacement as the closest rail node. Nodes of the same color are coupled vertically for one time step.

Interaction solvers come in various modifications [2, 3]. In the closed solution system of ANSYS two approaches were taken. The first is to couple the two systems.

At any given time step by the application of constraint equations a bond is formed between the nodes representing the wheel of the train and the closest located node of the rails. Only the vertical degrees of freedom are bonded not to transmit any numerically generated horizontal acceleration, which stems from the forward shifts of the train in each time step. After the solver has found the equilibrium for the given time step the bonds are removed, the train is shifted forward and new constrain equations are defined to the closest nodes of the rail in this newly updated position. Then the next time step is solved. In Figure 9 a sketch of the solution procedure is shown. Figure 10 shows the resulting position at time step number 150 which means the train has already moved forward 10m (dt=0.002s).

It is noteworthy, that the aforementioned solution procedure is valid only until no loss of contact occurs between the interacting systems. Once the wheel forces change direction to uplift, clearly the solution becomes incorrect. However, to verify the corectness of the solver while contact is maintaned an alternative uncoupled, iterative solver has been developed. In this approach the two systems (train and

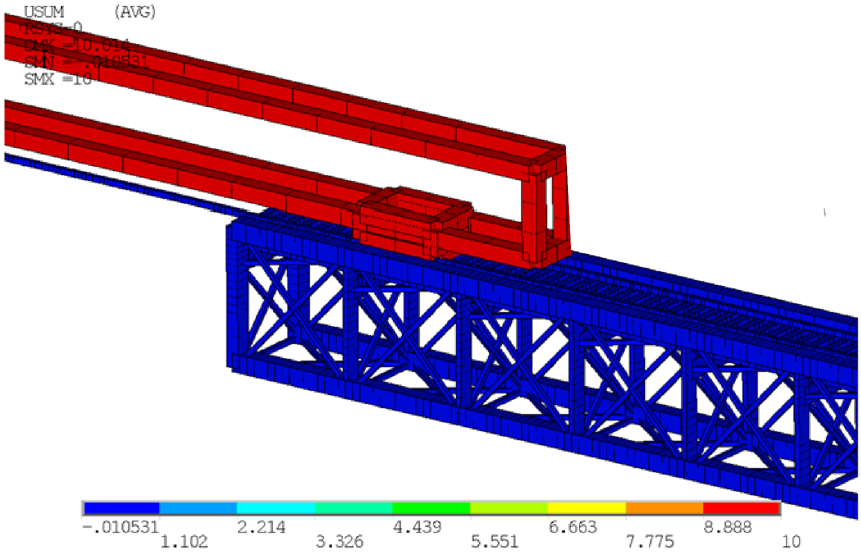

Figure 10: Showing the position of the train in time step 150.

bridge) are not connected in any degrees of freedom but influence each other by trasmittion of interaction forces on the wheels and the resulting displacements of the rails. At any given time step first the train forces are computed on a supported train system. In a second solution the wheel contact forces are applied on the rail, which then yields the rail deformations. This is the end of one iteration step. The resulting deformations are then applied to the supports of the train to compute an updated set of wheel forces which in turn are applied to the track. Iterations are repeated until convergence is reached. Afterwards, the train is moved forward. This analysis is extremely time consimung as the analysis has to be restarted after each partial solution and so information exchange must be realized through files saved on the hard drive. For these reasons only a short time of the train passing was analysed to compare the two solvers. Figure 11 shows this comparison.

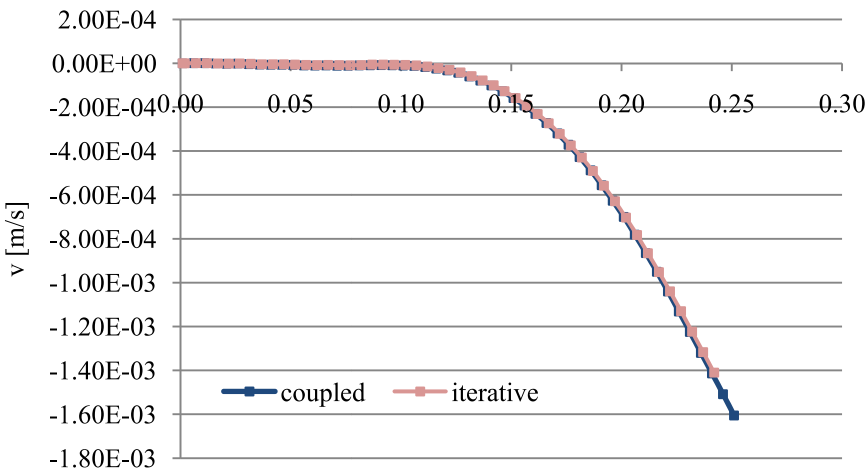

Figure 11: Comparison of the two solvers for train-track interaction.

In getting the correct response in time, independent of the solver, the initial conditions play a crucial role. For the described analysis the train starts off in level position acquired from its own weight. No impulse, i.e. initial velocity or acceleration was applied to the carriages. The static displacement of the carriages due to self-weight is about 52cm. Care must be taken in properly defining an initial time step. In this step we want to let the train reach its nonzero vertical displacement but introduce zero velocity and acceleration. This can be achieved by running the first step as steady-state in two substeps with time integration turned off. After establishing such an initial step the time integration can be turned on and carried out over the required time frame.

4 Results

4.1 Rainflow Counting

For computing the fatigue curves the rainflow counting [4] algorithm was used. The algorithm has several stages. First peaking is performed. In this phase the signal is cleared of intermediate values between local peaks which are defined by the change of the slope of the curve. In the second phase filtering is done, however not in the traditional sense, simply values below a threshold are eliminated. It is to get rid of unwanted small perturbations and noise. Finally the actual rainflow counting is performed. The procedure counts full and half loops based on the criteria of inter-relation of four points in the series (see Figure 12). In the end classes are set up based on their desired number and the number of cycles for each class is determined. Half-loops are counted as ½ cycle.

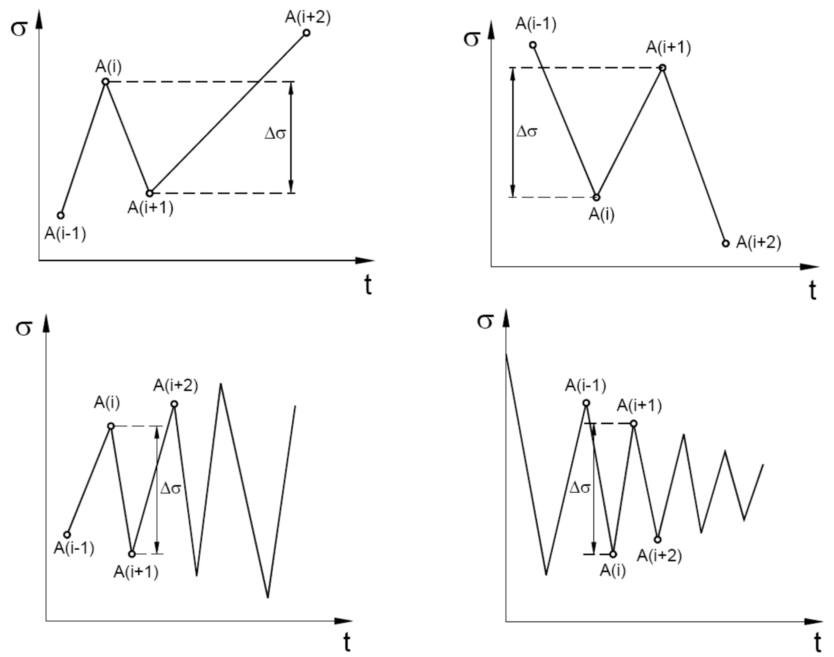

Figure 12: Rainflow counting of full and half cycles.

The time history analysis outcome exported in terms of stresses was ready to be processed by the rainflow counting algorithm. The threshold for the filtering was chosen 0.1% of the maximum amplitude. The cycle counts for a typical day are plotted in Figure 13. The preparation of the signal for the cycle counting does have its nuances. An engineering judgment on the peaking and filtering is advisory. As the peaking and filtering greatly depend on the sampling of the data intermediate checks are beneficial to the final results.

4.2 Fatigue

What one must have in mind is that the filtering of the data should not affect the overall extremes and thus should yield consistently the same classes regardless of the filtering threshold. The cycles counted for the select day are presented in 10 classes. The positive behaviour of the processing is that the low magnitude cycles are greatly affected by increasing the threshold value while with higher cycle magnitudes this effect decreases.

From observations the approximate number of trains that pass over the bridge per day could be extrapolated. We estimated 53 trains crossing the bridge in a day. With the shear stress records from the numerical analysis cycle counts for both investigated cross-girder joints were computed.

Originally the numerical model of the bridge lacked some stiffening plates exactly at the problematic joints. The results for this initial case are given here first.

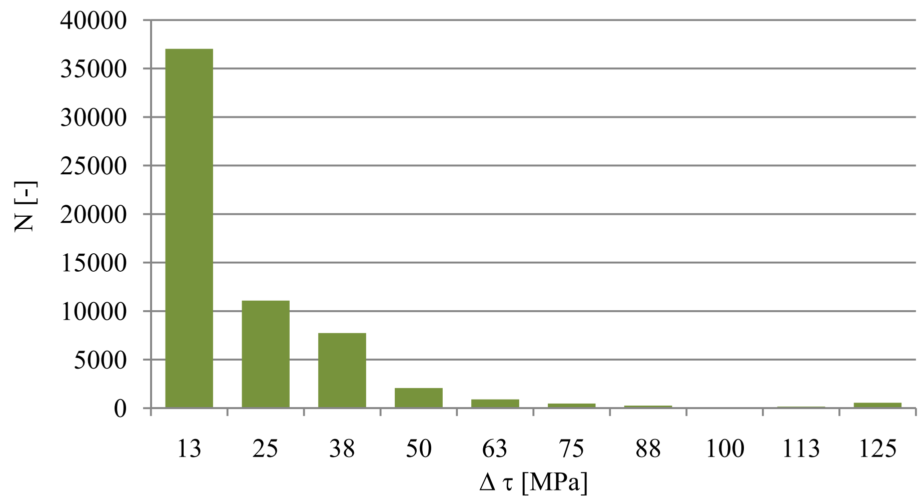

Figure 13: Cycle counts by rainflow algorithm on one typical day. East cross-girder; filtering threshold 0.1%.

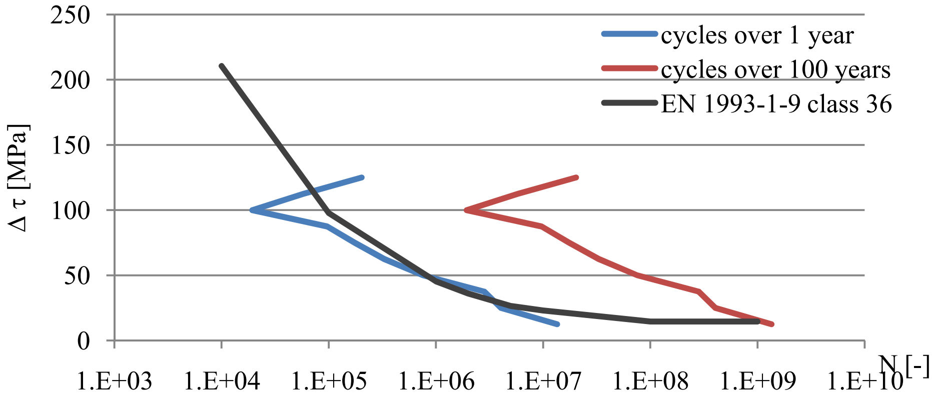

Figure 14: N-S curve for the joint compared to class 36 (EN 1993-1-9); east cross-girder – initial model.

At this point it seemed that the fracture of the cross-beam at the joint could have suffered from bad detailing. Simply calculating the maximum shear stresses in the cross-girders in the damaged region appeared to support this conclusion. For mild steels of the era we have found the yield strengths of f_y = 240MPa (1922) and f_y =370MPa (1908). If we assume the lower value of the two we arrive at the unequality

$$\tau_{Ed} \leq \frac{f_y}{\sqrt{3} \cdot \gamma_{M0}}, \text{ with } \gamma_{M0} = 1.0 \,,$$
$$134 \text{ MPa} \leq 138.5 \text{ MPa}.$$

This equates to a safety factor of 1.036. The requirement is very close to the material strength and assuming that heavier freight trains have operated on the line the limit strength of the material could have been exceeded.

However, upon closer examination of the original blueprints additional stiffening plates were found at the joint. Its inclusion does decrease the overall stress ranges at the joint. These results follow here.

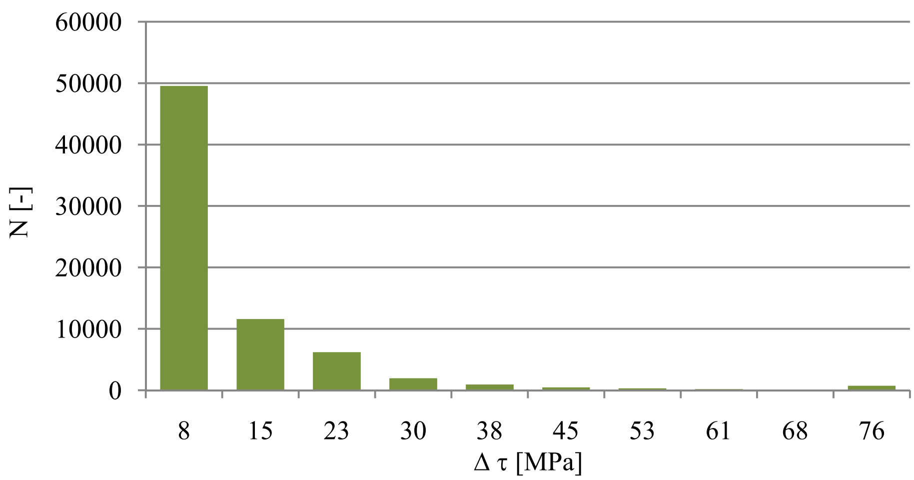

Figure 15: Cycle counts for one day. East cross-girder, dt=0.002s.

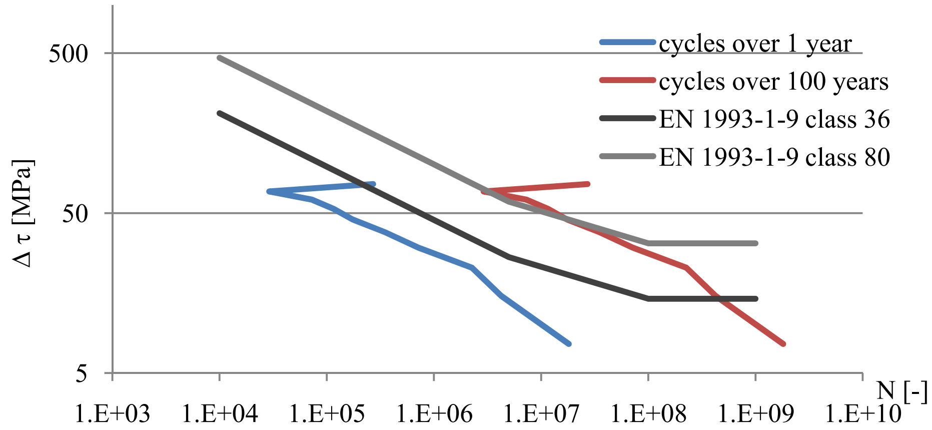

Figure 16: N-S curve for the joint compared to class 80 (EN 1993-1-9); east cross-girder – final model; dt=0.002s.

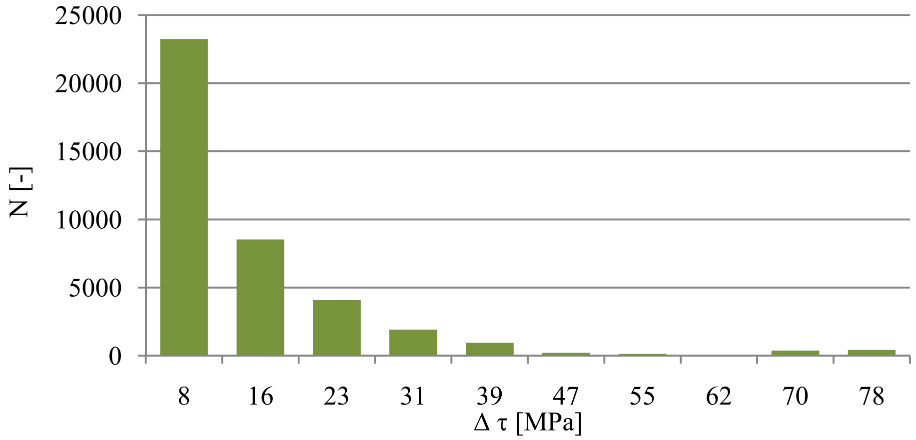

Figure 17: Cycle counts for one day. East cross-girder, dt=0.005s.

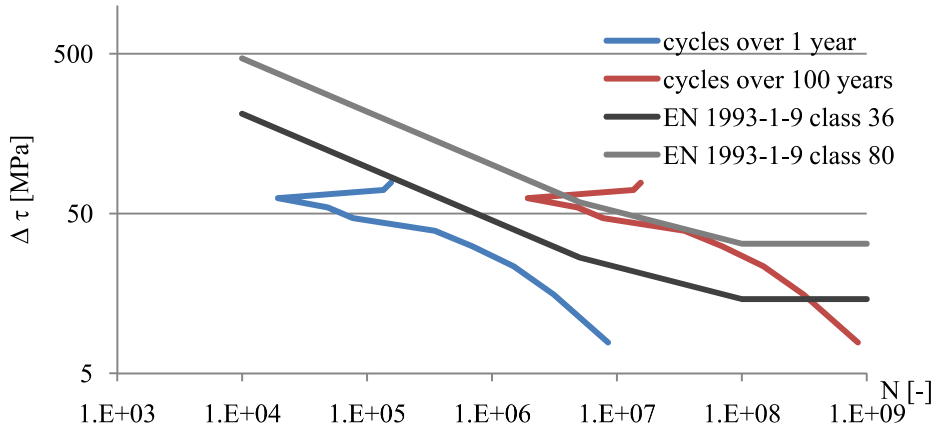

Figure 18: N-S curve for the joint compared to class 80 (EN 1993-1-9); east cross-girder – final model; dt=0.005.

Finally, the cycles calculated from numerical data can be matched with normative restrictions [6]. For this task the joint is assumed to be of class 80 and the computed cycle counts are taken from Figure 15 and Figure 17. In the presented figures one can see that the one year cycle counts do not touch curve from the code as in the case of the initial model. By assuming a life expectancy of one hundred years and adding up the cycles over this time period one can see that this final curve reaches the normative curve for class 80. This leads us to believe that fatigue could have caused cracking of the element at the joint.

Moreover, we may state that the difference in time stepping is not significant. The smaller time step of 0.002 seconds gives more low level perturbations, which can be filtered out, however these are not critical for the fatigue assessment of the joint. Nonetheless, for a fatigue assessment of this type a time step of 0.005 seconds is apparently sufficient.

5 Remarks

The Salzach Bridge is an old riveted bridge. It has had some cracks on its cross-girders for about 20 years. They were mitigated by the standard method of hole drilling. It is unclear what caused this damage. The two forerunning candidates are incompetent detailing or fatigue. An initial analysis pointed rather towards an erroneous design of the detail. Nonetheless, additional investigation showed that the answer is not clearly straightforward and that fatigue could have played a more or less significant role in the development of the damage. Thinking about the inaccuracies in the loading history of the bridge no definitive statements can be made about the damaged joints. On the other hand the global model is not in the state to provide in depth stress distributions on the joint. Therefore a detailed numerical model of the joint is planned to assess stress distribution in the damaged joints more precisely. Applying both static and dynamic load cases to such a model could shed more light on the problem.

Acknowledgment

The European Commission’s Research Fund for Coal and Steel is thankfully acknowledged for supporting the presented research activity.

References

[1] C. Esveld, A.W.M. Kok, „Interaction between moving vehicles and railway track at high speed“, Rail Engineering International, 27, 3, 14-16, 1998.

[2] I. Faria, R. Delgado, R. Calçada, ”Bridge-vehicles dynamic interaction: numerical modelling and practical applications”, Bridges for High-Speed Railways, 159-179, 2008.

[3] K. Liu, E. Reynders, G De Roeck, G. Lombaert, “Experimental and numerical analysis of a composite bridge for high-speed trains”, Journal of Sound and Vibration 320, 201-220, 2009.
[4] D. Ribeiro, R. Calçada, R. Delgado, “Fatigue on metallic railway bridges: Methodology of analysis and application to Alcácer do Sal Bridge”, IABMAS, Porto, Portugal, 2006.
[5] C. Vale, N. Ribeiro, R. Calçada, R. Delgado, “Dynamics of a precast system for high-speed railway tracks”, COMPDYN, 3rd ECCOMAS, Corfu, Greece, May 2011.
[6] Eurocode 3: Design of steel structures, Part 1-9: Fatigue.